Characterization of Guanylate Cyclase Activity in Single Retinal Rod Outer Segments

Y. KOUTALOS,* K. NAKATANI,‡ T. TAMURA,* and K.-W. YAU*§‖

From the Departments of *Neuroscience and §Ophthalmology and ‖Howard Hughes Medical Institute, The Johns Hopkins University School of Medicine, Baltimore, Maryland 21205; and ‡Institute for Biological Sciences, University of Tsukuba, Tsukuba, Ibaraki 305, Japan

ABSTRACT cGMP mediates vertebrate phototransduction by directly gating cationic channels on the plasma membrane of the photoreceptor outer segment. This second messenger is produced by a guanylate cyclase and hydrolyzed by a light-activated cGMP-phosphodiesterase. Both of these enzyme activities are Ca^{2+} sensitive, the guanylate cyclase activity being inhibited and the light-activated phosphodiesterase being enhanced by Ca^{2+}. Changes in these activities due to a light-induced decrease in intracellular Ca^{2+} are involved in the adaptation of photoreceptors to background light. We describe here experiments to characterize the guanylate cyclase activity and its modulation by Ca^{2+} using a truncated rod outer segment preparation, in order to evaluate the enzyme's role in light adaptation. The outer segment of a tiger salamander rod was drawn into a suction pipette to allow recording of membrane current, and the remainder of the cell was sheared off with a probe to allow internal dialysis. The cGMP-gated channels on the surface membrane were used to monitor conversion of GTP, supplied from the bath, into cGMP by the guanylate cyclase in the outer segment. At nominal 0 Ca^{2+}, the cyclase activity had a K_m of 250 μM MgGTP and a V_{max} of 25 μM cGMP s^{-1} in the presence of 1.6 mM free Mg^{2+}; in the presence of 0.5 mM free Mg^{2+}, the K_m was 310 μM MgGTP and the V_{max} was 17 μM cGMP s^{-1}. The stimulation by Mg^{2+} had an EC_{50} of 0.2 mM Mg^{2+} for MgGTP at 0.5 mM. Ca^{2+} inhibited the cyclase activity. In a K^+ intracellular solution, with 0.5 mM free Mg^{2+} and 2.0 mM GTP, the cyclase activity was 13 μM cGMP s^{-1} at nominal 0 Ca^{2+}; Ca^{2+} decreased this activity with a IC_{50} of ~90 nM and a Hill coefficient of ~2.0.

INTRODUCTION

Visual transduction takes place in the outer segments of retinal rod and cone photoreceptors. In this process, photoisomerization of the visual pigment activates a biochemical cascade that leads to stimulation of the cGMP-phosphodiesterase and hence the hydrolysis of guanosine 3′:5′-cyclic monophosphate (cGMP; for recent

Address correspondence to Dr. Yiannis Koutalos, Department of Physiology, Box C-240, University of Colorado School of Medicine, 4200 E. Ninth Ave., Denver, CO 80262.

T. Tamura's present address is Department of Ophthalmology, Kanazawa University School of Medicine, 13-1 Takara-machi, Kanazawa, Ishikawa 920, Japan.

J. GEN. PHYSIOL. © The Rockefeller University Press · 0022-1295/95/11/863/28 $2.00
Volume 106 November 1995 863–890

reviews see Lagnado and Baylor, 1992; Detwiler and Gray-Keller, 1992; Pugh and Lamb, 1993; Koutalos and Yau, 1993; Yarfitz and Hurley, 1994; Yau, 1994). In the dark, cGMP binds to and opens cation channels on the plasma membrane of the outer segment (for review see Yau and Baylor, 1989). These open channels sustain an inward dark current, which partially depolarizes the cell. In the light, the cGMP level decreases and the cation channels close to produce a membrane hyperpolarization as the light response.

Ca^{2+} also plays an important role in phototransduction. In darkness, there is a steady influx of Ca^{2+} into the outer segment through the cGMP-gated channels, balanced by an efflux through a $Na^+/Ca^{2+},K^+$ exchanger (Yau and Nakatani, 1984; Cervetto, Lagnado, Perry, Robinson, and McNaughton, 1989). In the light, the closure of the cGMP-gated channels stops the Ca^{2+} influx, but the efflux continues, causing a decrease in the free Ca^{2+} concentration in the outer segment (Yau and Nakatani, 1985*a*; McNaughton, Cervetto, and Nunn, 1986; Lagnado, Cervetto, and McNaughton, 1992; Gray-Keller and Detwiler, 1994; McCarthy, Younger, and Owen, 1994). This decrease in Ca^{2+} triggers a negative feedback to produce light adaptation (Matthews, Murphy, Fain, and Lamb, 1988; Nakatani and Yau, 1988*c*; Matthews, Fain, Murphy, and Lamb, 1990; see also Matthews, 1995). This feedback involves multiple Ca^{2+} targets in the phototransduction pathway. First, the rod guanylate cyclase, which synthesizes cGMP, is inhibited by Ca^{2+} (Koch and Stryer, 1988; Kawamura and Murakami, 1989; Gorczyca, Gray-Keller, Detwiler, and Palczewski, 1994*a*; Gorczyca, Van Hooser, and Palczewski, 1994*b*; see also Miller and Korenbrot, 1994), so that when Ca^{2+} decreases in the light the enzymatic activity increases, counteracting the light-stimulated phosphodiesterase activity. Second, low Ca^{2+} diminishes the light-activated phosphodiesterase activity by facilitating rhodopsin phosphorylation, which promotes deactivation of rhodopsin (Kawamura and Murakami, 1991; Palczewski, Rispoli, and Detwiler, 1992; Kawamura, 1993; Gray-Keller, Polans, Palczewski, and Detwiler, 1993; Chen and Hurley, 1994; Chen, Makino, Peachey, Baylor, and Simon, 1995); in addition, there may be a second Ca^{2+} target in this regulatory pathway (Lagnado and Baylor, 1994). Finally, Ca^{2+} decreases the apparent affinity of the cGMP-gated channel for cGMP (Hsu and Molday, 1993; Gordon and Zimmerman, 1994; Chen, Illing, Molday, Hsu, Yau, and Molday, 1994; Nakatani, Koutalos, and Yau, 1995), so that when Ca^{2+} falls in the light, the channels tend to reopen despite the decrease in cGMP concentration.

In an attempt to understand the relative contributions from the separate Ca^{2+} regulatory pathways to the sensitivity of rods to light, we have undertaken a quantitative characterization of each of these pathways. In this article, we describe measurements of the guanylate cyclase activity and its dependence on Ca^{2+}. Although such measurements have previously been made by others (Koch and Stryer, 1988; Koch, 1991; Gorczyca et al., 1994*a*), our experiments were carried out on single, semiintact rod outer segments, so that the cyclase activity could be measured under ionic conditions and protein concentrations close to the physiological situation. We used the truncated rod outer segment preparation (Yau and Nakatani, 1985*b*; Nakatani and Yau, 1988*b*), which allows recording of membrane current from the outer segment and at the same time manipulation of the internal ionic conditions. Guanosine 5′-triphosphate (GTP) was dialyzed into the truncated outer segment,

and its conversion into cGMP was monitored by the cGMP-gated channels on the plasma membrane.

Preliminary accounts of the work have appeared in Koutalos, Nakatani, and Yau (1992, 1993).

METHODS

Larval tiger salamanders (*Ambystoma tigrinum*) (Charles D. Sullivan, Nashville, TN) were used in all of the experiments. Each animal was decapitated and pithed under dim red light. All subsequent steps were carried out in infrared light with the help of image converters. The enucleated eyes were hemisected, and the retinas were isolated and kept at room temperature for up to several hours in Ringer's solution containing 110 mM NaCl, 2.5 mM KCl, 1.6 mM $MgCl_2$, 1 mM $CaCl_2$, 5 mM TMA-HEPES (tetramethylammonium hydroxide–4-(2-hydroxyethyl) l-piperazineethanesulfonic acid), and 5 mM glucose, pH 7.55. Isolated rod cells were obtained by chopping a piece of retina on Sylgard (Dow Corning Corp., Midland, MI), under Ringer's solution, with a razor blade.

Suction pipettes for recording membrane current from rod outer segments were made from Corning 7740 borosilicate glass capillaries (A-M Systems, Everett, WA) and coated with tri-*n*-butylchlorosilane (Pfaltz and Bauer Inc., Waterbury, CT), as described previously (Baylor, Lamb, and Yau, 1979; Lamb, McNaughton, and Yau, 1981). A truncated rod outer segment was obtained by drawing the outer segment of a rod cell partially into a suction pipette and then shearing off the remainder of the cell with a glass probe made from the same capillaries. In this way, the interior of the outer segment could be dialyzed with the bath solution. The membrane potential was held at 0 mV.

For most of the experiments, K^+ was absent in both the pipette and the bath solutions in order to eliminate the $Na^+/Ca^{2+},K^+$ exchange activity, which requires K^+ to function (Cervetto et al., 1989). Several pairs of pipette/bath solutions were used: (*a*) For the characterization of the cGMP-gated channel dose–response relation, the pipette contained Ringer's solution and the bath a choline chloride (ChCl) solution (110 mM ChCl, 1.6 mM free Mg^{2+}, 2 mM TMA-ethylene glycol-bis(β-aminoethyl ether) *N,N,N′,N′*-tetraacetic acid (TMA-EGTA), 5 mM TMA-HEPES, and 5 mM glucose, pH 7.55) containing 0.5 mM 3-isobutyl-1-methxanthine (IBMX) and different concentrations of cGMP (Na^+ salt). (*b*) For the dependence of the cyclase activity on GTP, the pipette contained a modified Ringer's solution without Ca^{2+} (110 mM NaCl, 1.6 or 0.5 mM free Mg^{2+}, 2 mM TMA-EGTA, 5 mM TMA-HEPES, and 5 mM glucose, pH 7.55) and the bath a ChCl solution (110 mM ChCl, 1.6 or 0.5 mM free Mg^{2+}, 2 mM TMA-EGTA, 5 mM TMA-HEPES, and 5 mM glucose, pH 7.55) containing 0.5 mM IBMX and different concentrations of GTP (Na^+ salt) or cGMP. Ca^{2+} was kept low in the pipette solution in order to eliminate Ca^{2+} influx through the cGMP-gated channels. (*c*) For studying the Mg^{2+} effect on the cyclase, the pipette contained a modified Ringer's solution without any divalents (110 mM NaCl, 2 mM TMA-EGTA, 2 mM TMA-EDTA, 5 mM TMA-HEPES, and 5 mM glucose, pH 7.55), so as to eliminate both Ca^{2+} and Mg^{2+} influx, and the bath a ChCl solution (110 mM ChCl, 2 mM TMA-EGTA, 5 mM TMA-HEPES, and 5 mM glucose, pH 7.55) containing 0.5 mM IBMX and different concentrations of cGMP or GTP and free Mg^{2+} (see formula below). (*d*) For studying the Ca^{2+} modulation of the cyclase, the pipette contained a modified Ringer's solution with low Ca^{2+} (110 mM NaCl, 1.6 or 0.5 mM free Mg^{2+}, 2 mM bis(o-amino phenoxy)ethene-*N,N,N′,N′*-tetraacetic acid (BAPTA), 0 nominal or 0.001 mM free Ca^{2+}, 5 mM TMA-HEPES, and 5 mM glucose, pH 7.55) and the bath a ChCl solution (110 mM ChCl, 1.6 or 0.5 mM free Mg^{2+}, 2 mM BAPTA, 5 mM TMA-HEPES, and 5 mM glucose, pH 7.55) containing 0.5 mM IBMX, GTP, or cGMP, as well as different concentrations of free Ca^{2+} (see formula below). In some experiments, adenosine 5′-triphosphate (ATP; Na^+ salt) or inorganic pyrophosphate (PP_i) was also added. (*e*) For studying the Ca^{2+} modulation of the cyclase in the presence of a physiological K^+ concentration in the outer segment, the pipette contained a low Ca^{2+}–ChCl solution (110 mM ChCl, 0.5 mM free Mg^{2+}, 2 mM BAPTA, 0.001 mM free

Ca^{2+}, 5 mM TMA-HEPES, and 5 mM glucose, pH 7.55) and the bath a K^+–gluconate solution (110 mM K^+-gluconate, 0.5 mM free Mg^{2+}, 2 mM BAPTA, 5 mM TMA-HEPES, and 5 mM glucose, pH 7.55) containing 0.5 mM IBMX, GTP, or cGMP, and different concentrations of free Ca^{2+}. In this case, since there was no Na^+ in the pipette and only small amounts of Na^+ in the bath, the Na^+/Ca^{2+}, K^+ exchange activity should also be negligible. In the above solutions, the choice of nominal 0 or low buffered Ca^{2+} in the extracellular solution had no significance; the Ca^{2+} dependence of the cyclase is the same with either of these two Ca^{2+} concentrations in the pipette. For solution pairs A to D, the recorded membrane current was inward, being carried by Na^+; for solution pair E, the recorded current was outward, being carried by K^+.

The total concentrations $[Mg]_{total}$ and $[Ca]_{total}$ of Mg^{2+} and Ca^{2+} (as chloride salts) to be added in order to give the desired free concentrations $[Mg]_{free}$ and $[Ca]_{free}$ were calculated according to the formulas

$$[Mg]_{total} = [Mg]_{free} + \sum_{chelator} [Mg]_{chelator} \quad (1)$$

$$[Ca]_{total} = [Ca]_{free} + \sum_{chelator} [Ca]_{chelator}, \quad (2)$$

where $[Mg]_{chelator}$ and $[Ca]_{chelator}$ are the Mg^{2+} and Ca^{2+} concentrations bound to a particular chelator. The chelators were EGTA, BAPTA, GTP, ATP, and PP_i, and the concentrations of chelator-complexed Mg^{2+} and Ca^{2+} were given by

$$[Mg]_{EGTA} = \frac{407.65 \times [Mg]_{free}}{2862.4 + 407.65 \times [Mg]_{free} + 93.4 \times [Ca]_{free}} \times [EGTA] \quad (3a)$$

$$[Ca]_{EGTA} = \frac{93.4 \times [Ca]_{free}}{2862.4 + 407.65 \times [Mg]_{free} + 93.4 \times [Ca]_{free}} \times [EGTA] \quad (3b)$$

$$[Mg]_{BAPTA} = \frac{0.059 \times [Mg]_{free}}{1.084 + 0.059 \times [Mg]_{free} + 0.0093 \times [Ca]_{free}} \times [BAPTA] \quad (4a)$$

$$[Ca]_{BAPTA} = \frac{0.0093 \times [Ca]_{free}}{1.084 + 0.059 \times [Mg]_{free} + 0.0093 \times [Ca]_{free}} \times [BAPTA] \quad (4b)$$

$$[Mg]_{GTP} = \frac{10.47 \times [Mg]_{free}}{1.11 + 10.47 \times [Mg]_{free}} \times [GTP] \quad (5)$$

$$[Mg]_{ATP} = \frac{11.6 \times [Mg]_{free}}{1.12 + 11.6 \times [Mg]_{free}} \times [ATP] \quad (6)$$

$$[Mg]_{PP_i} = \frac{294.7 \times [Mg]_{free}}{9.85 + 294.7 \times [Mg]_{free} + 0.0003 \times [Ca]_{free}} \times [PP_i] \quad (7a)$$

$$[Ca]_{PP_i} = \frac{0.0003 \times [Ca]_{free}}{9.85 + 294.7 \times [Mg]_{free} + 0.0003 \times [Ca]_{free}} \times [PP_i]. \quad (7b)$$

In the above equations all concentrations are millimolar, except for $[Ca]_{free}$, which is nanomolar. The concentration of each chelator, [chelator], designates the total chelator added. For EGTA or BAPTA the total concentration was always 2.0 mM, for PP_i, 100 μM, and for ATP, 2.0 mM; for GTP it was varied according to the experiment. The formulas were derived on the basis of the pub-

lished association constants for BAPTA (Tsien, 1980), EGTA, GTP, ATP, and PP_i (Martell and Smith, 1974), and at a pH of 7.55, corresponding to a H^+ concentration of $10^{-7.44}$ M (see Martell and Smith, 1974). The binding of Ca^{2+} to GTP and ATP is negligible in the Ca^{2+} concentration range used in the experiments and was ignored.

Changes of bath solution were effected by a system of pneumatically controlled valves, and the solution bathing the truncated end of the outer segment was changed in ~300 ms (Nakatani and Yau, 1988*a*). The experiments were carried out in darkness and at room temperature. Electrical records were low-pass filtered (DC to 30–100 Hz). In all of the figures, inward membrane current is plotted as negative. Junction currents have been subtracted from all records.

RESULTS

Relation between cGMP-gated Channel Activation and cGMP Concentration

To measure the rod guanylate cyclase activity, we used the cGMP-gated channels on the plasma membrane as a monitor of the cGMP concentration in the outer segment. For this purpose, it was first necessary to obtain the relation between the activation of these channels and cGMP concentration under similar experimental conditions. Fig. 1 *A* shows membrane currents elicited from a truncated rod outer seg-

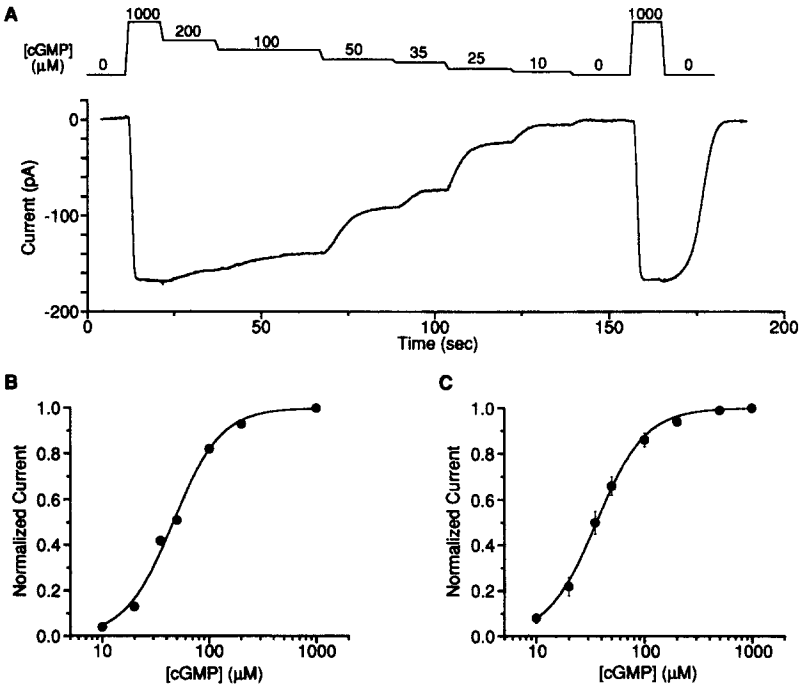

FIGURE 1. (*A*) Membrane currents elicited by different concentrations of cGMP from a truncated salamander rod outer segment. The pipette contained Ringer's and the bath a ChCl solution. (*B*) Normalized currents from *A* are plotted as a function of the cGMP concentration. The solid curve is drawn according to Eq. 8a with $K_{1/2}$ = 46 μM and n = 1.9. (*C*) Collected results from five rod outer segments. The solid curve is $K_{1/2}$ = 36 μM and n = 1.9.

ment by different concentrations of cGMP, in the presence of 0.5 mM IBMX, which inhibited the basal phosphodiesterase activity (see Koutalos et al., 1995). In this experiment, normal Ringer's solution was in the pipette while a ChCl solution was used for intracellular dialysis (see solution pair A in Methods). After normalization with respect to the saturated current (J_{max}) elicited by 1 mM cGMP, the current is plotted against cGMP concentration in Fig. 1 *B*. The smooth curve is a least-squares fit according to the Hill equation

$$j = \frac{J}{J_{max}} = \frac{[cG]^n}{[cG]^n + K_{1/2}{}^n}, \tag{8a}$$

where J is the current elicited by a concentration [cG]of cGMP, j is the normalized current, $K_{1/2}$ is the half-saturating cGMP concentration, and n the Hill coefficient. For this cell, $K_{1/2}$ = 46 μM cGMP and n = 1.9. The averaged results from five rods gave $K_{1/2}$ = 36 μM cGMP and n = 1.9 (Fig. 1 *C*). The saturated current, J_{max}, varied from 60 to 240 pA in the five experiments. This variation in the saturated current has also been observed in previous work (Nakatani and Yau, 1988*b*) and does not seem to correlate with the length of the truncated rod outer segment. The averaged $K_{1/2}$ and n values above were used for converting current to cGMP concentration in all other experiments, according to

$$[cG] = K_{1/2}\left(\frac{1}{j} - 1\right)^{-1/n}. \tag{8b}$$

The cGMP concentration, [cG], defined by Eq. 8b, is an empirical experimental parameter, which is useful for calculating the guanylate cyclase activity but does not necessarily correspond to a constant cGMP concentration inside the truncated rod outer segment. It is rather a measure of the overall cGMP concentration inside the outer segment, as sensed by the current. Near saturation, any uncertainty in the current would lead to a large uncertainty in the empirical cGMP concentration. For this reason, we have restricted our analysis to j values <0.9.

Measurement of Guanylate Cyclase Activity and Its Dependence on GTP

To measure the guanylate cyclase activity and its dependence on substrate concentration, we supplied GTP from the bath and let it be converted into cGMP inside the truncated rod outer segment by the enzyme. Fig. 2 *A* shows the currents elicited from a truncated rod by different concentrations of GTP. In this experiment, the pipette contained a modified Ringer's solution with nominal 0 Ca^{2+} and 0.5 mM free Mg^{2+}, whereas a ChCl solution with nominal 0 Ca^{2+}, 0.5 mM free Mg^{2+}, and 0.5 mM IBMX was used for intracellular dialysis (solution pair B in Methods). The lower divalent cation concentrations in the pipette account for the generally larger cGMP-induced current (see also Figs. 5 and 6) compared with that in Fig. 1. Since MgGTP, and not GTP, is the actual substrate, we have chosen to plot the GTP-elicited currents and the cyclase activity as a function of the MgGTP concentration. In this way, a separate effect of Mg^{2+} on the cyclase, independent of its role as the GTP cofactor, can be identified (see Fig. 4). The GTP-elicited current, normalized by the saturated current activated by 1 mM cGMP, is plotted against MgGTP

concentration in Fig. 2 *B*. These currents can be converted to cGMP concentrations according to Eq. 8b and plotted as such in Fig. 2 *C* (*right ordinate*).

In steady state (i.e., at the current plateau), the rate of cGMP synthesis equals the rate of cGMP loss due to diffusion out of the outer segment. The rate of cGMP loss is shown below to be proportional to the steady state cGMP concentration in the outer segment, with a proportionality constant r that can be measured. Thus, we can write

$$\alpha = r[\mathrm{cG}] \tag{9}$$

where α is the cyclase activity and [cG] is given by Eq. 8b. For this outer segment $r = 0.4\ \mathrm{s}^{-1}$ (see below), and from Eqs. 8b and 9 we can calculate the guanylate cyclase activity. The enzyme activities derived in this way are plotted on the left ordinate in Fig. 2 *C*. The smooth curve is the Hill equation

$$\alpha(z) = \frac{V_{\max} z^{h}}{z^{h} + K_{m}{}^{h}}. \tag{10}$$

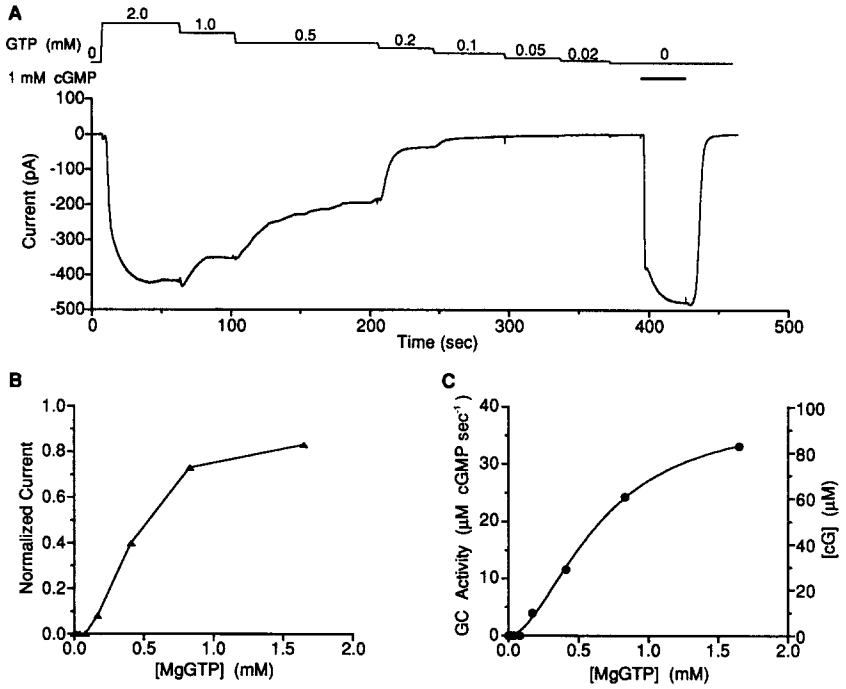

FIGURE 2. (*A*) Membrane currents elicited by different GTP concentrations from a truncated salamander rod outer segment. The pipette contained a modified Ringer's solution with nominal 0 Ca^{2+}, and the intracellular solution contained 0.5 mM free Mg^{2+}. (*B*) Normalized GTP-elicited current from *A* plotted as a function of MgGTP concentration. The MgGTP concentrations were different from the indicated GTP concentrations in *A* because at 0.5 mM free Mg^{2+} not all of the GTP is Mg^{2+} bound. (*C*) Currents from *B* converted to cGMP concentrations. Right *y*-axis is guanylate cyclase activity in micromolar cGMP. Left *y*-axis is guanylate cyclase (*GC*) activity in micromolar cGMP s^{-1}, obtained by multiplying the cGMP concentrations by r (0.4 s^{-1}). The smooth curve is a least-squares fit with Eq. 10, with $V_{max} = 39$ μM cGMP s^{-1}, $K_m = 640$ μM MgGTP, and $h = 1.8$.

where z is the MgGTP concentration. The fitted values are V_{max} = 39 μM cGMP s^{-1}, K_m = 640 μM MgGTP and h = 1.8.

Fig. 3 shows the measurement of the parameter r. In Fig. 3 *A*, the decay of the cGMP-elicited current shown in Fig. 2 *A* (right end of the trace) is displayed on an expanded time scale; in Fig. 3 *B*, the current is converted to cGMP concentration and plotted on a logarithmic scale. As the linearity of the latter plot shows, the decay of cGMP is a first-order process over a large part of its time course, a feature also expected from diffusion theory (see Appendix). The slope of the decline gives r = 0.4

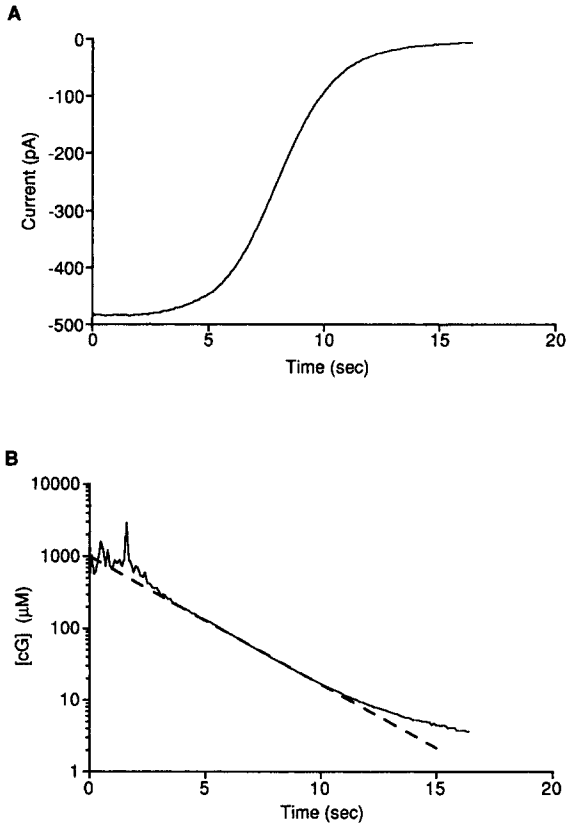

FIGURE 3. Measurement of the rate constant r for the rod outer segment in Fig. 2. (*A*) Expanded record of the decay of the current elicited by 1 mM cGMP from Fig. 2 *A*. The bath solution was switched to 0 cGMP at time zero. (*B*) Decay of the cGMP concentration, obtained by conversion from the current in *A* and plotted in semilog scales. The straight line has slope r = 0.4 s^{-1}.

s^{-1} (mean ± SD = 0.29 ± 0.11 s^{-1} from 41 cells). The deviation at later times may be due to a slight baseline drift, but perhaps not to cGMP buffering (see Koutalos et al., 1995). The cGMP concentrations encountered in the measurements of guanylate cyclase activity described in this paper lie mostly within the range where the decline is exponential (10–200 μM), thus justifying the use of Eq. 9. The derivation of Eq. 9 depends on the assumption that the concentration of cGMP produced in the outer segment is spatially homogeneous. Since cGMP diffuses out of the outer segment, however, its concentration should follow a longitudinal gradient, decreasing to zero at the open end. Nonetheless, despite this spatial gradient, calculations

based on diffusion theory (see Appendix) indicate that Eq. 9 provides a good approximation of the cyclase activity under our experimental conditions.

Fig. 4 shows collected results for the dependence of the guanylate cyclase activity on MgGTP concentration. The open circles show averaged enzyme activity as a function of the MgGTP concentration in 0.5 mM free Mg^{2+} (four cells). The error bars indicate standard errors. The dashed curve is a Hill equation fit (Eq. 10), giving V_{max} = 17 μM cGMP s^{-1}, K_m = 310 μM MgGTP, and h = 2.6. Averaged results in 1.6 mM free Mg^{2+} are also shown (*filled triangles*; eight cells), giving V_{max} = 25 μM cGMP s^{-1}, K_m = 250 μM MgGTP, and h = 1.4 (*solid curve*). The amount of the guanylate cyclase in the outer segment is ~1/100th that of rhodopsin (Koch, 1991), which is equivalent to a cytoplasmic concentration of ~60 μM, assuming that about half of the rod outer segment is free cytosolic space. This concentration gives turnover numbers of 0.4 and 0.3 s^{-1} in 1.6 and 0.5 mM free Mg^{2+}, respectively. The difference in the Hill coefficient at the two Mg^{2+} concentrations may not be reliable, because of the limited MgGTP concentrations used and the very small currents at low MgGTP concentrations. On the other hand, the differences in V_{max} and K_m are quite clear, suggesting an effect of Mg^{2+} on the cyclase in addition to its association with GTP as substrate. Finally, based on the analysis outlined in the Appendix, the V_{max} and K_m values obtained here may be overestimated by ~20%.

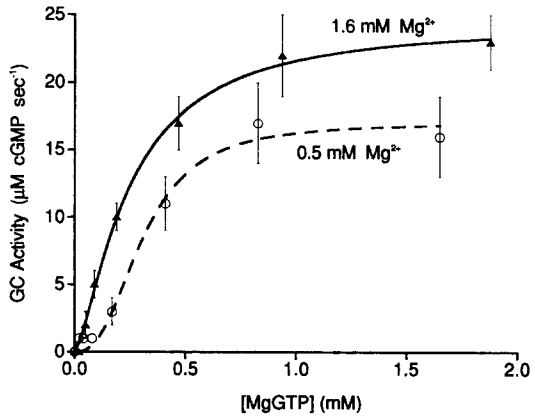

FIGURE 4. Average guanylate cyclase activity as a function of MgGTP concentration at 1.6 mM (*filled triangles*; eight cells) and 0.5 mM (*open circles*; four cells) free Mg^{2+}. The smooth curves are least-squares fits according to Eq. 10, with V_{max} = 25 μM cGMP s^{-1}, K_m = 250 μM MgGTP, and h = 1.4 (*solid curve*), and V_{max} = 17 μM cGMP s^{-1}, K_m = 310 μM MgGTP, and h = 2.6 (*dashed curve*).

Effect of Mg^{2+} on Guanylate Cyclase

We have examined the effect of free Mg^{2+} on guanylate cyclase more closely. Since divalent cations have a blocking effect on the cGMP-gated channel under the solution arrangement in these experiments, we first had to measure this blockage by Mg^{2+} in order to make corrections. Fig. 5 *A* shows the current, $J([Mg])$, elicited by 1 mM cGMP at different Mg^{2+} concentrations. In this experiment, the pipette contained a modified Ringer's solution with nominal 0 Ca^{2+} and 0 Mg^{2+}, whereas a ChCl solution containing nominal 0 Ca^{2+}, 0.5 mM IBMX, 0 or 1 mM cGMP, and different Mg^{2+} concentrations was used for intracellular dialysis (solution pair C in Methods). The initial current transient in the trace is due to the channels responding to cGMP be-

fore the full Mg^{2+} block occurred. After normalization with respect to the current in 0 Mg^{2+}, $J(0)$, the currents $j([Mg]) = J([Mg])/J(0)$ are plotted against free Mg^{2+} concentrations in Fig. 5 *B*. The smooth curve is a least-squares fit according to

$$j([Mg]) = \frac{K_b^{\,q}}{[Mg]^q + K_b^{\,q}} \tag{11}$$

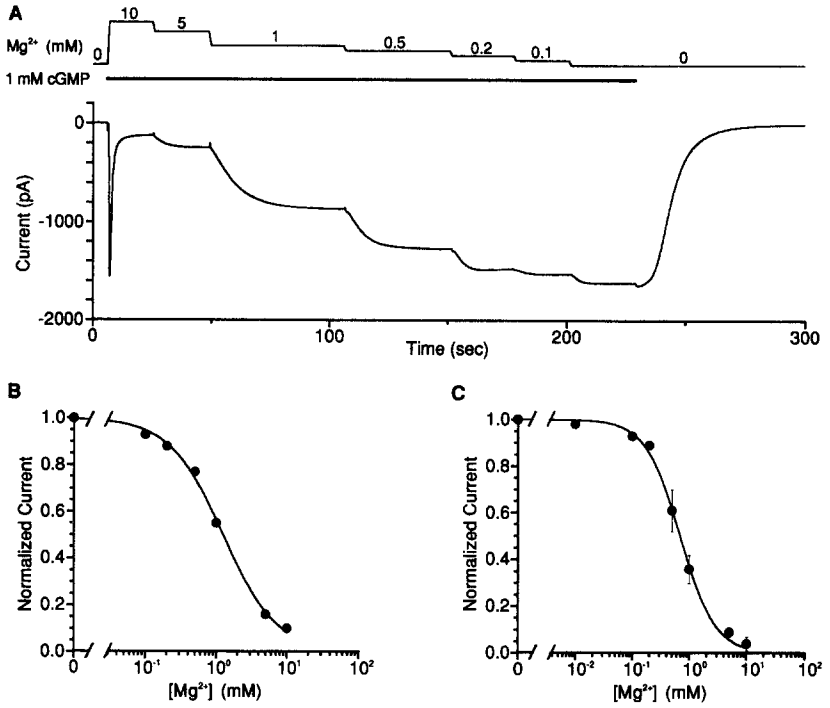

FIGURE 5. (*A*) Mg^{2+} block of the cGMP-elicited current from a salamander rod outer segment. The pipette contained a modified Ringer's solution with nominal 0 Ca^{2+} and 0 Mg^{2+}. (*B*) Normalized currents from *A* plotted against the free Mg^{2+} concentrations. Curve fit is Eq. 11, with K_b = 1.3 mM Mg^{2+} and q = 1.1. (*C*) Collected results from six rod outer segments. Curve fit is Eq. 11, with K_b = 0.7 mM Mg^{2+} and q = 1.4.

with K_b = 1.3 mM Mg^{2+} and q = 1.1. Fig. 5 *C* shows averaged results from six cells with the same curve fit, giving K_b = 0.7 mM Mg^{2+} and q = 1.4. These values are broadly consistent with the results obtained from excised-patch measurements (Zimmerman and Baylor, 1992). The Mg^{2+} block is largely independent of the cGMP concentration (Karpen, Brown, Stryer, and Baylor, 1993), so the above numbers should be valid at lower cGMP concentrations as well. They were used to correct for the Mg^{2+} block in the following cyclase experiments.

Fig. 6 *A* shows the currents elicited by GTP at different free Mg^{2+} concentrations. Solution pair C was again used in this experiment. The GTP and Mg^{2+} concentra-

tions were adjusted to give the desired free Mg^{2+} concentration, while maintaining the MgGTP concentration constant at 0.5 mM, with the exception that in nominal 0 Mg^{2+} solution the GTP concentration was arbitrarily chosen to be 1.0 mM. The GTP-induced currents, again normalized by the saturated current elicited by 1 mM cGMP, are plotted against the free Mg^{2+} concentrations in Fig. 6 *B*. At Mg^{2+} concentrations < ~0.5 mM, the GTP-induced current increased with increasing free Mg^{2+} concentration, indicating a stimulating effect of Mg^{2+} on the cyclase. At

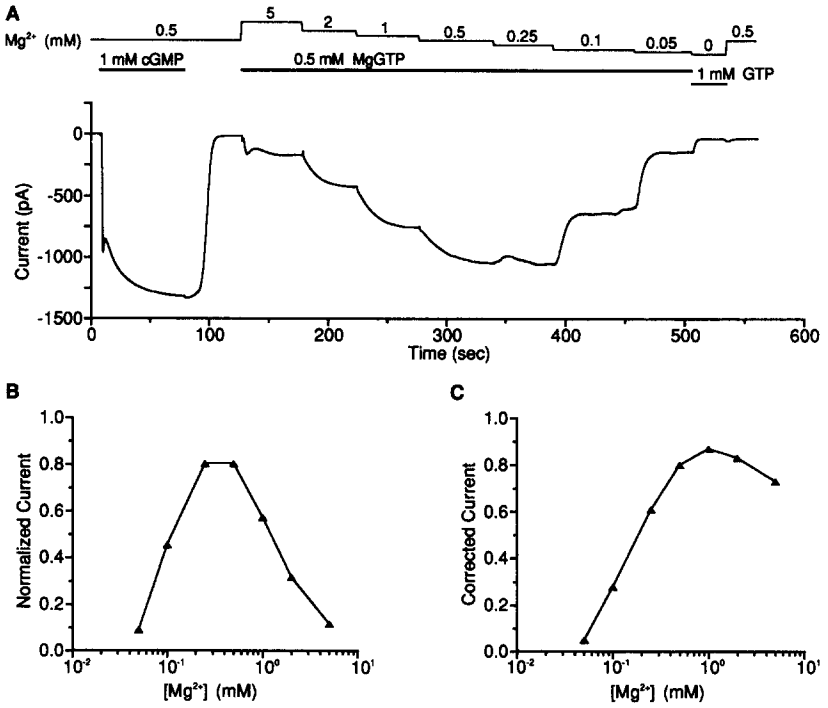

FIGURE 6. (*A*) Dependence of the GTP-elicited current on the free Mg^{2+} concentration. The pipette contained a modified Ringer's solution with nominal 0 Ca^{2+} and 0 Mg^{2+}. The bath GTP concentration was adjusted to keep the MgGTP concentration constant at 0.5 mM. (*B*) Normalized currents from *A* plotted against the free Mg^{2+} concentrations. (*C*) Currents from *B* after correction for the blocking effect of Mg^{2+} on the channels.

higher Mg^{2+} concentrations, however, the current decreased with increasing Mg^{2+}, consistent with the blocking effect of Mg^{2+} on the channel. To correct for channel block at different Mg^{2+} concentrations, these currents were converted to the equivalent currents at 0.5 mM free Mg^{2+} according to Eq. 11, and replotted in Fig. 6 *C*. This plot shows an enhancing effect of Mg^{2+} on the cyclase activity up to ~1 mM Mg^{2+}. The inhibition at higher Mg^{2+} concentrations may be genuine or due to an undercorrection of the Mg^{2+} block. Fig. 7 *A* shows a plot of the same data, but with the currents converted to cGMP concentrations according to Eq. 8b (*right ordinate*).

The constant r for this outer segment was 0.35 s^{-1}, giving cyclase activities indicated on the left ordinate. Averaged results from five cells are shown in Fig. 7 *B*. For simplicity, we assumed that the cyclase activity plateaus at high Mg^{2+} concentrations and fitted a Hill equation to the data, giving an EC_{50} of 0.2 mM Mg^{2+} and a Hill coefficient of 1.8. Though these numbers are expected to show some dependence on the MgGTP concentration (see Fig. 4), they nonetheless provide a general indication of how the cyclase activity varies with Mg^{2+} at nonsaturating substrate concentrations.

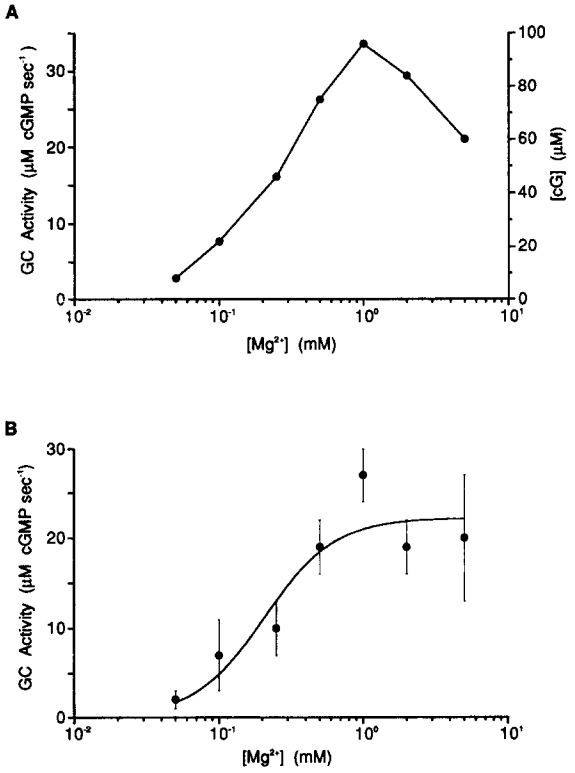

FIGURE 7. (*A*) Guanylate cyclase (*GC*) activity, calculated from the currents in Fig. 6 *C*. The two *y*-axes give the cyclase activity in micromolar cGMP (*right*) and micromolar cGMP s^{-1} (*left*). (*B*) Average guanylate cyclase activity (five cells) as a function of the free Mg^{2+} concentration in 0.5 mM MgGTP. The solid line is a least-squares fit according to the Hill equation, with an EC_{50} of 0.2 mM Mg^{2+} and a Hill coefficient of 1.8.

Effect of Ca^{2+} on Guanylate Cyclase

Our next experiment was to examine the effect of Ca^{2+} on cyclase activity. Fig. 8 *A* shows the influence of increasing the Ca^{2+} concentration from 0 to 100 nM on the GTP-induced current. In this experiment, the pipette contained a modified Ringer's solution with nominal 0 Ca^{2+} and 1.6 mM free Mg^{2+}, whereas a ChCl solution containing 0.5 mM IBMX, 1.6 mM free Mg^{2+}, and different GTP and Ca^{2+} concentrations was used for intracellular dialysis (solution pair D in Methods). With 2 mM GTP, the current was hardly affected when Ca^{2+} was increased from nominal 0 to 100 nM (channel blockage due to 100 nM Ca^{2+} is negligible). With 0.2 mM GTP, on the other hand, the current was reduced by about a factor of two with the same solution change. After normalization against the saturated current elicited by 1

mM cGMP, the currents at the above and other GTP concentrations were plotted in Fig. 8 *B*, with filled triangles indicating 0 Ca^{2+} and open circles indicating 100 nM Ca^{2+}. The same results are plotted in the form of guanylate cyclase activity in Fig. 8 *C*, using a measured r value of 0.3 s^{-1}. The smooth curves are least-squares fits according to the Hill equation, with V_{max} taken to be the same (24 μM cGMP s^{-1}) for nominal 0 and 100 nM Ca^{2+}. 100 nM Ca^{2+} shifts the K_m from 340 to 480 μM

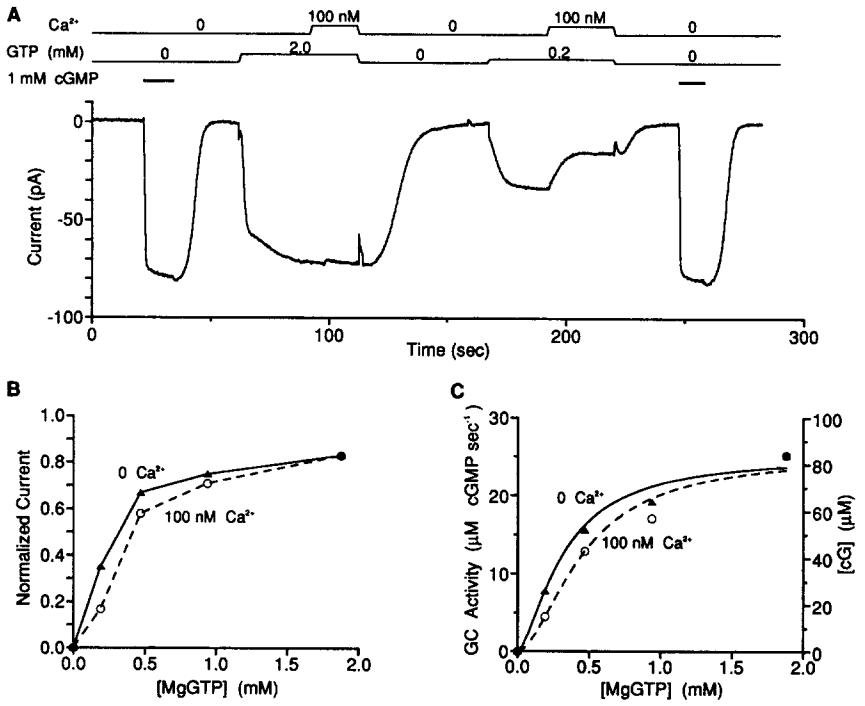

FIGURE 8. (*A*) Effect of 100 nM Ca^{2+} on the currents elicited by 2.0 mM and 0.2 mM GTP in a truncated salamander rod outer segment. The pipette contained a modified Ringer's solution with nominal 0 Ca^{2+}. The free Mg^{2+} concentration in the intracellular solution was 1.6 mM. (*B*) Normalized currents from *A*, together with those at 1.0 and 0.5 mM GTP, plotted against MgGTP concentrations. Filled triangles show nominal 0 Ca^{2+}; open circles represent 100 nM Ca^{2+}. (*C*) Guanylate cyclase activity, obtained from the currents in *B*, plotted against MgGTP concentration. Filled triangles are nominal 0 Ca^{2+}; open circles show 100 nM Ca^{2+}. The two *y*-axes give the cyclase activity in micromolar cGMP (*right*) and micromolar cGMP s^{-1} (*left*). The smooth curves were drawn according to Eq. 10, with V_{max} = 24 μM cGMP s^{-1}, K_m = 340 μM MgGTP, and h = 1.5 (*solid curve*), and V_{max} = 24 μM cGMP s^{-1}, K_m = 480 μM MgGTP, and h = 1.7 (*dashed curve*).

Mg-GTP. Averaged results from three cells at 1.6 mM free Mg^{2+} are shown in Fig. 9 *A*. The shift in the K_m of the enzyme due to 100 nM Ca^{2+} is from ~400 to 615 μM. We have also carried out experiments at 0.5 mM free Mg^{2+}, with the averaged results from three cells shown in Fig. 9 *B*. In this case, the shift in K_m due to 100 nM Ca^{2+} is from ~350 to 610 μM MgGTP. At both Mg^{2+} concentrations, there was a

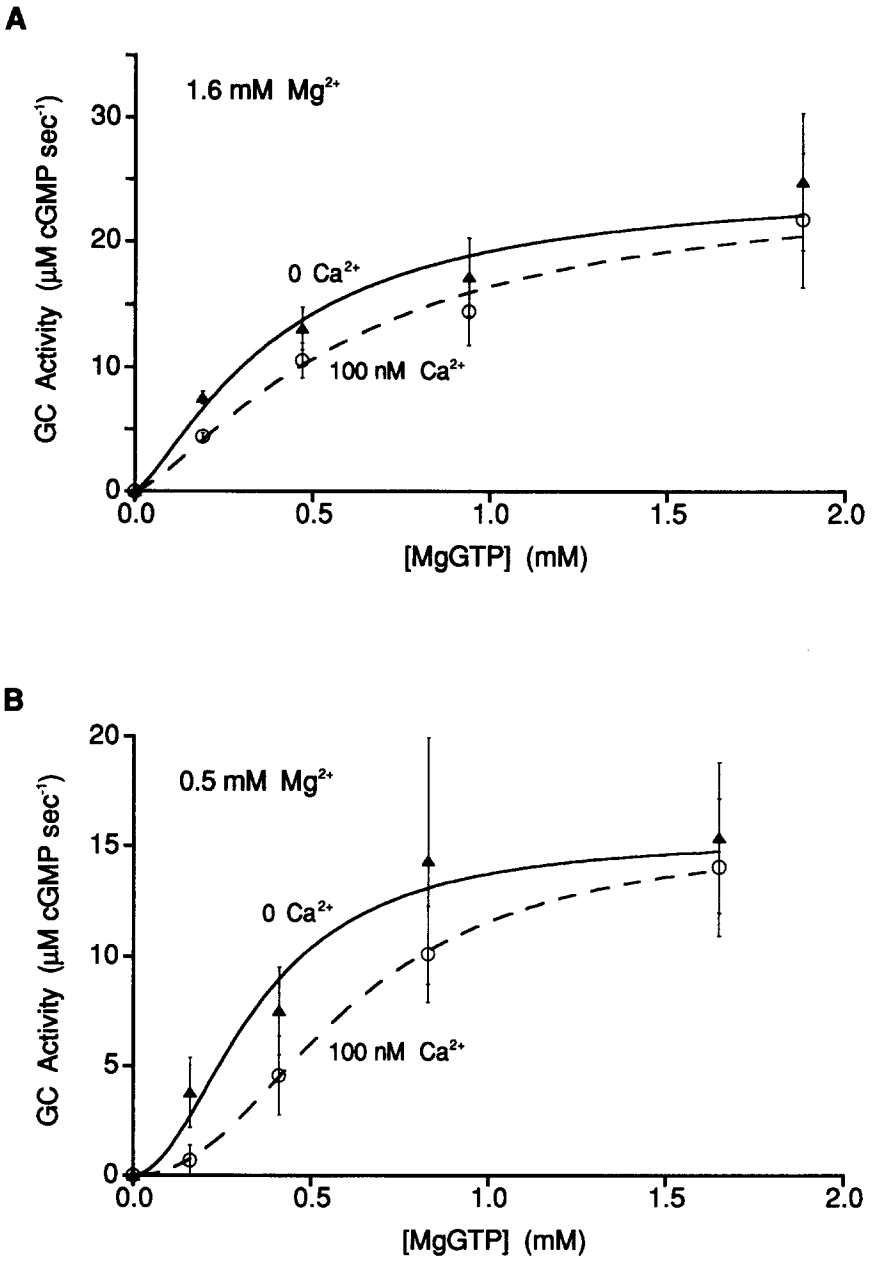

FIGURE 9. Averaged results for the effect of 100 nM Ca^{2+} on guanylate cyclase activity. (*A*) 1.6 mM free Mg^{2+}. Filled triangles represent nominal 0 Ca^{2+}; open circles are 100 nM Ca^{2+}. Curves are Eq. 10, with V_{max} = 25 μM cGMP s^{-1}, K_m = 400 μM MgGTP, and h = 1.4 (*solid curve*), and V_{max} = 25 μM cGMP s^{-1}, K_m = 615 μM MgGTP, and h = 1.4 (*dashed curve*). (*B*) 0.5 mM free Mg^{2+}. Filled triangles show nominal 0 Ca^{2+}; open circles represent 100 nM Ca^{2+}. Curves are Eq. 10, with V_{max} = 15 μM cGMP s^{-1}, K_m = 350 μM MgGTP, and h = 2.0 (*solid curve*), and V_{max} = 15 μM cGMP s^{-1}, K_m = 610 μM MgGTP, and h = 2.2 (*dashed curve*).

clear inhibition of the cyclase activity by 100 nM Ca^{2+} only at the lowest GTP concentration used, that is, 0.2 mM. At higher GTP concentrations, the effect of 100 nM Ca^{2+} was rather insignificant, suggesting that the inhibition by Ca^{2+} is competitive with respect to GTP.

We went on to examine the cyclase activity over a broader range of Ca^{2+} concentrations. We have tested three separate conditions: 0.2 mM GTP/0.5 mM free Mg^{2+}, 0.5 mM GTP/0.5 mM free Mg^{2+}, and 2.0 mM GTP/1.6 mM free Mg^{2+}. Fig.

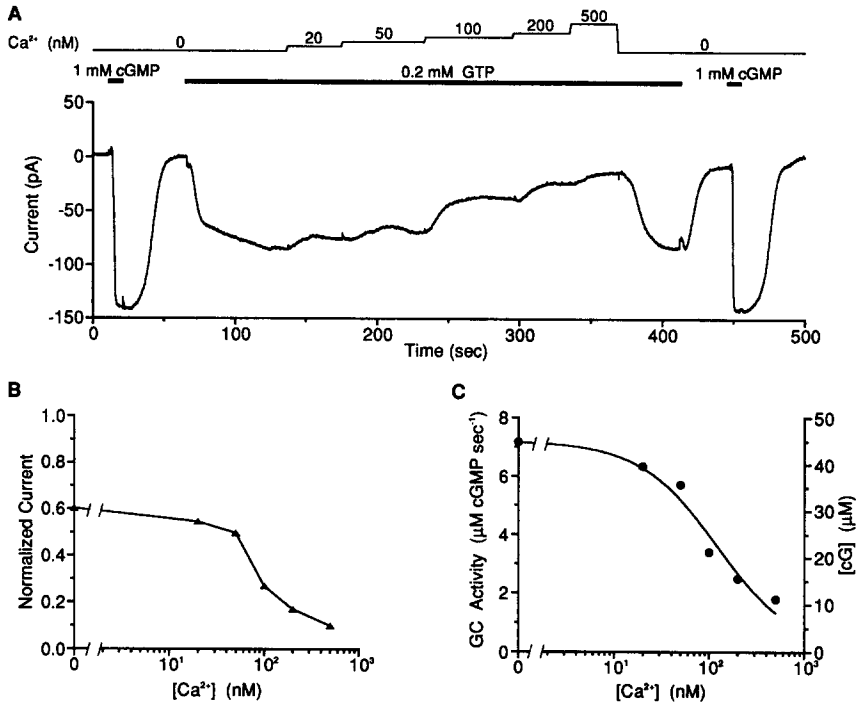

FIGURE 10. (*A*) Effect of Ca^{2+} on the current elicited by 0.2 mM GTP from a truncated salamander rod outer segment. The pipette contained a modified Ringer's solution with nominal 0 Ca^{2+}. The intracellular solution contained 0.5 mM free Mg^{2+}. (*B*) Normalized currents from *A* plotted against Ca^{2+} concentrations. (*C*) Currents from *B* converted to guanylate cyclase activity. The two *y*-axes give the cyclase activity in micromolar cGMP (*right*) and micromolar cGMP s^{-1} (*left*). Curve fit is according to the Hill equation, with an IC_{50} of 120 nM Ca^{2+} and a Hill coefficient of 1.1.

10 *A* shows an experiment with the first condition. The pipette and the intracellular dialysis solutions were the same as in Fig. 8 *A* (solution pair D in Methods). The normalized currents from Fig. 10 *A* are plotted against the Ca^{2+} concentration in Fig. 10 *B*, with the corresponding cyclase activities shown in Fig. 10 *C* (using a measured r value of 0.16 s^{-1}). A Hill equation fit gives a half-maximal inhibition at 120 nM Ca^{2+} and a Hill coefficient of 1.1. Averaged results from three cells under the same conditions are shown in Fig. 11 (*filled triangles*). To facilitate comparisons, the

enzyme activity in each experiment has been normalized to unity at nominal 0 Ca^{2+}. In the same figure we have included the data from the two other conditions: 0.5 mM GTP/0.5 mM free Mg^{2+} (*open circles*, five cells) and 2.0 mM GTP/1.6 mM free Mg^{2+} (*filled circles*, four cells). The absolute cyclase activities at nominal 0 Ca^{2+} are 12, 17, and 24 μM cGMP s^{-1} for 0.2, 0.5, and 2 mM GTP, respectively. These values are broadly consistent with the results shown in Fig. 4, although the value in 0.2 mM GTP is substantially higher, which we ascribe to data scatter at low activation of the channels. The smooth curves in Fig. 11 are least-squares fits according to the Hill equation, giving half-inhibition constants/Hill coefficients of 70 nM Ca^{2+}/1.8,

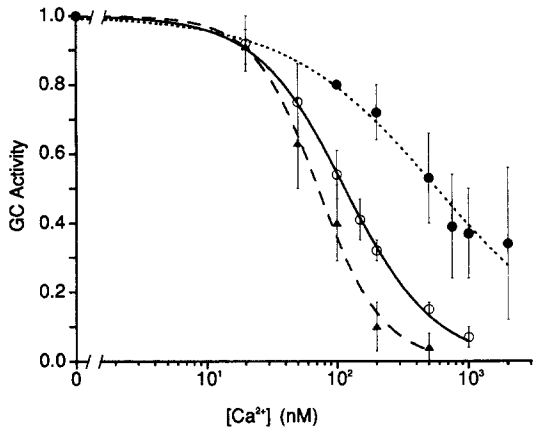

FIGURE 11. Collected results on guanylate cyclase activity as a function of Ca^{2+} concentration at different GTP and free Mg^{2+} concentrations. In all cases, a ChCl solution was used for intracellular dialysis. For each set of data, the activity has been normalized over the value at nominal 0 Ca^{2+}. Closed circles represent 2.0 mM GTP/1.6 mM free Mg^{2+}; open circles are 0.5 mM GTP/0.5 mM free Mg^{2+}; filled triangles are 0.2 mM GTP/0.5 mM free Mg^{2+}. The smooth curves are least-squares fits according to the Hill equation, with IC_{50}/Hill coefficient of 570 nM Ca^{2+}/0.8, 115 nM Ca^{2+}/1.3, and 70 nM Ca^{2+}/1.8, respectively. The activities at nominal 0 Ca^{2+} were 24, 17, and 12 μM cGMP s^{-1}, respectively.

115 nM Ca^{2+}/1.3, and 570 nM Ca^{2+}/0.8 for the three conditions. The increase of the half-inhibition constant with increasing GTP concentration is again qualitatively consistent with a competitive inhibition of the cyclase by Ca^{2+}.

Finally, we have examined Ca^{2+} modulation in the presence of ATP or PP_i. For these experiments we have used 0.5 mM GTP and 0.5 mM free Mg^{2+}. With 2.0 mM ATP, the half-inhibition constant was 100 nM Ca^{2+} (three cells, data not shown), not significantly different from that in the absence of ATP. Likewise, 100 μM PP_i did not affect the cyclase activity either in nominal 0 or 100 nM Ca^{2+} (three cells, data not shown).

Ca^{2+} Modulation of Guanylate Cyclase in a K^+ Intracellular Solution

In the experiments described so far, a ChCl intracellular solution was used for intracellular dialysis. Since K^+ is physiologically the predominant intracellular cation, we decided to repeat some of the experiments using a K^+ solution for dialysis. In these experiments, the pipette contained a ChCl solution with 1 μM free Ca^{2+} and 0.5 mM free Mg^{2+}, and a K^+–gluconate solution containing 0.5 mM IBMX, 0.5 mM

free Mg^{2+}, and the appropriate cGMP, GTP, and Ca^{2+} concentrations was used for intracellular dialysis (solution pair E in Methods). In this case, the current was outward, carried by K^+. The choice of 1 μM instead of nominal 0 Ca^{2+} in the extracellular solution again had no significance. Fig. 12 *A* shows one such experiment with 0.5 mM GTP. As before, the GTP-induced current decreased with increasing Ca^{2+} concentration. The normalized currents are plotted against Ca^{2+} concentrations in Fig. 12 *B* and converted to cyclase activity in Fig. 12 *C* (with $r = 0.2\ s^{-1}$ for this ex-

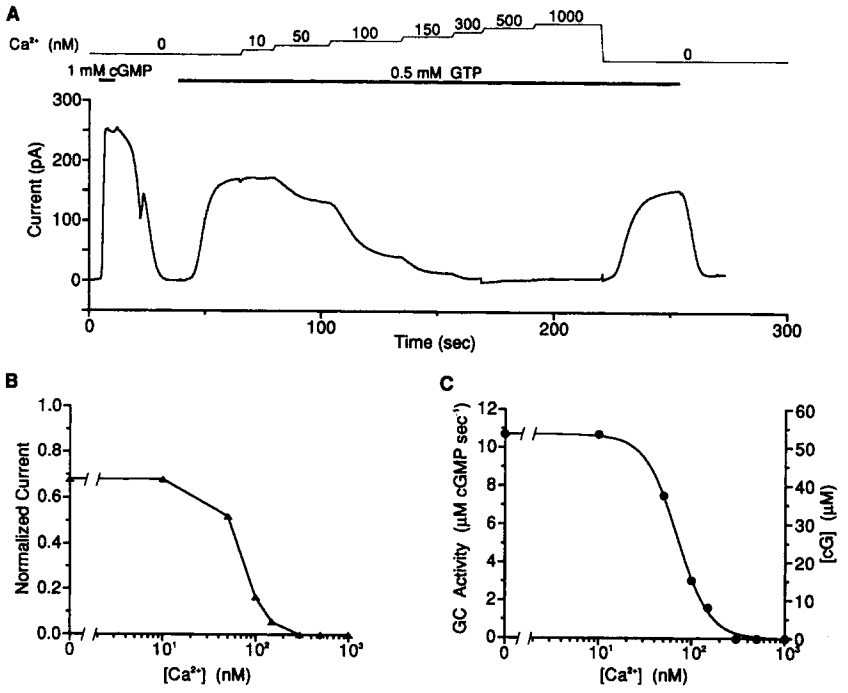

FIGURE 12. (*A*) Effect of Ca^{2+} on the current elicited with 0.5 mM GTP from a truncated salamander rod outer segment. The pipette contained a ChCl solution, and the intracellular solution contained 110 mM K^+ and 0.5 mM free Mg^{2+}. (*B*) Normalized currents from *A* plotted against Ca^{2+} concentrations. (*C*) Currents from *B* converted to guanylate cyclase activity. The two *y*-axes give the cyclase activity in micromolar cGMP (*right*) and micromolar cGMP s^{-1} (*left*). Curve fit is according to the Hill equation, giving an IC_{50} of 70 nM Ca^{2+} and a Hill coefficient of 2.5.

periment). A Hill equation fit to the points (*smooth curve*) gives a half-inhibition constant of 70 nM Ca^{2+} and a Hill coefficient of 2.5. Averaged results from four cells are shown in Fig. 13 (*open circles*). In the same plot, data from four other cells with 2 mM GTP are also shown (*filled triangles*). The averaged cyclase activity at nominal 0 Ca^{2+} was 8 μM cGMP s^{-1} for 0.5 mM GTP and 13 μM cGMP s^{-1} for 2 mM GTP, again in broad agreement with the data shown in Fig. 4. The smooth curves are Hill equation fits to the points, giving a half-inhibition constant of 59 nM Ca^{2+} and a Hill coefficient of 1.7 for 0.5 mM GTP, and 87 nM Ca^{2+} and 2.1 for 2.0 mM

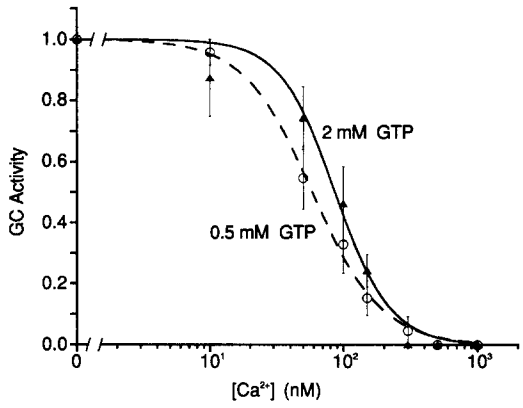

FIGURE 13. Collected results on the Ca^{2+} dependence of guanylate cyclase activity with a K^+ intracellular solution and 0.5 mM free Mg^{2+}. Open circles represent 2.0 mM GTP; filled triangles are 0.5 mM GTP. For each set of data, the activity has been normalized over the value at nominal 0 Ca^{2+}. The curves are least-squares fits according to the Hill equation, with IC_{50}/Hill coefficient of 87 nM Ca^{2+}/2.1 and 57 nM Ca^{2+}/1.7, respectively. The activities at nominal 0 Ca^{2+} were 13 and 8 μM cGMP s^{-1}, respectively.

GTP. The increase in the half-inhibition constant for Ca^{2+} with increasing GTP concentration is not as large as in the experiments with the ChCl intracellular solution, perhaps suggesting an effect of K^+ on the cyclase. In biochemical preparations, K^+ has been shown to stimulate cyclase activity (Fleischman and Denisevich, 1979; Hakki and Sitaramayya, 1990).

DISCUSSION

We have characterized the biochemical activity of rod guanylate cyclase and its dependence on Ca^{2+} by recording electrically from a single rod outer segment. The advantage of our method is that enzyme activity is measured in conditions close to the physiological situation.

In our experiments, the steady state velocity of the GTP cyclization reaction was measured, in contrast to the common biochemical procedure, which measures initial velocity. One concern of a steady state measurement is that the cyclase may be inhibited by the reaction end products, namely, cGMP and PP_i. We have not examined the effect of cGMP, because exogenous cGMP would interfere with the measurement of the current elicited by GTP. However, biochemical experiments (Hakki and Sitaramayya, 1990) have not shown any significant inhibition of the cyclase by cGMP at concentrations as high as 800 μM, which is much higher than would be encountered in our experiments. On the other hand, PP_i has been reported to inhibit guanylate cyclase activity (Hakki and Sitaramayya, 1990; Hayashi and Yamazaki, 1991; Yang and Wensel, 1992). Using MgGTP as substrate, we did not find any effect of 100 μM PP_i on the cyclase in either nominal 0 or 100 nM Ca^{2+}. Since the calculated cGMP concentration in the rod outer segment produced by cyclase rarely exceeded 100 μM in our experiments, we can assume the same for PP_i. Thus, the observed Ca^{2+} effect on the cyclase does not appear to be through an inhibition of the inorganic pyrophosphatase activity, a possibility raised by Hakki and Sitaramayya (1990). Another possible concern about our experiments and

those of others (Koch and Stryer, 1988; Hakki and Sitaramayya, 1990) is the use of IBMX as an agent to inhibit cGMP-phosphodiesterase in order to measure cyclase activity. Recently, by studying the conversion of (S_p)-GTPαS into the hydrolysis-resistant (R_p)-cGMPS by rod guanylate cyclase, Gorczyca et al. (1994*b*) showed that IBMX also inhibits guanylate cyclase activity, with a K_i of ~1.5 mM. For competitive inhibition, this would suggest that IBMX at the concentration we used, 0.5 mM, may have increased the K_m of the guanylate cyclase by ~30%. We have not made any correction for this possible effect in our measurements.

The half-activation constant of 36 μM cGMP and the Hill coefficient of 1.9 for the opening of the channels by cGMP obtained in these experiments are in broad agreement with previous measurements from truncated toad rod outer segments (Nakatani and Yau, 1988*b*). They are also in broad agreement with measurements from excised patches (Fesenko, Kolesnikov, and Lyubarsky, 1985; Nakatani and Yau, 1985), though somewhat different values have also been reported (Zimmerman, Yamanaka, Eckstein, Baylor, and Stryer, 1985; Colamartino, Menini, and Torre, 1991). The half-maximal activation constant does not appear to be affected by IBMX, based on experiments with the hydrolysis-resistant cGMP analogue, 8′-bromo-cGMP (Nakatani and Yau, 1988*b*; see also Haynes and Yau, 1985). Recently, the half-activation constant for the channel has been found to be sensitive to Ca^{2+} (Hsu and Molday, 1993; Gordon and Zimmerman, 1994; Nakatani et al., 1995). However, this sensitivity to Ca^{2+} is lost in truncated rod outer segments after exposure to a nominal 0 Ca^{2+} intracellular solution for a few minutes (Nakatani et al., 1995). In all of the experiments described in this article, the outer segment was invariably dialyzed first with a nominal 0 Ca^{2+} solution for at least a few minutes after truncation, so we do not expect the modulation of the channel by Ca^{2+} to interfere with the measurement of the guanylate cyclase activity. At the same time, under our experimental conditions, we did not observe any progressive washout of the guanylate cyclase activating factor (Koch and Stryer, 1988; Gorczyca et al., 1994*a*), perhaps because the moderate ionic strength of all of the dialyzing solutions kept the factor membrane bound.

Biochemical measurements of bovine rod guanylate cyclase, with MnGTP as substrate, have given a K_m of 274 μM for the purified enzyme (Koch, 1991) and 230 μM for the partially solubilized enzyme (Hakki and Sitaramayya, 1990). Hayashi and Yamazaki (1991), also using MnGTP as substrate, obtained K_m's of 160 and 85 μM for two forms of guanylate cyclase purified from toad rod outer segments. In comparison, we have obtained a K_m of 310 μM MgGTP in 0.5 mM free Mg^{2+} and 250 μM MgGTP in 1.6 mM free Mg^{2+}. The enzyme turnover numbers for the purified enzyme range from 0.2–1.3 cGMP s^{-1} for the bovine enzyme (Koch, 1991) to 1–3 cGMP s^{-1} for the enzymes from toad (Hayashi and Yamazaki, 1991). The insensitivity of the purified enzyme to Ca^{2+} does not permit a useful comparison with our measurements. Moreover, the turnover number of 0.3–0.4 cGMP s^{-1} at nominal 0 Ca^{2+} we obtained has been calculated on the basis of a 60-μM enzyme concentration. If the concentration of the cyclase in the outer segment is lower (see Hayashi and Yamazaki, 1991), the turnover number will be proportionately higher. Finally, the enhancement of cyclase activity by free Mg^{2+} observed in our experiments, with a half-maximal effect at 0.2 mM, is in qualitative agreement with previous biochem-

ical measurements on the bovine enzyme, which arrived at a value of ~1.0 mM (Fleischman and Denisevich, 1979). In general, any agreement or disagreement between our measurements and the biochemical results should be interpreted with caution in view of species differences and radical differences in experimental conditions.

The physiological significance of the Mg^{2+} modulation of the cyclase is currently unclear. The free Mg^{2+} concentration has not been measured in rod outer segments, though, by analogy to other cell types, it is likely to be close to the 0.5–1.6 mM range that we used (see London, 1991). A light-induced decrease in the total Mg^{2+} content of rod outer segments has been reported (Somlyo and Walz, 1985), a situation also expected from the circulation of Mg^{2+} at the outer segment in darkness (Nakatani and Yau, 1988*a*). Nevertheless, the removal of external Mg^{2+} does not produce any obvious effect on the light response over a period of half a minute (Nakatani and Yau, 1988*a*).

Previously, Kawamura and Murakami (1989) also found an inhibition of the guanylate cyclase by Ca^{2+} in truncated rod outer segments. However, they did not measure the biochemical activity of the cyclase, and the Ca^{2+} dependence they obtained was from pooling experiments, each performed at a different dialyzing Ca^{2+} concentration. Thus, they were unable to derive a quantitative relation for the enzyme modulation by Ca^{2+}. Using 2 mM GTP and 12 mM total Mg^{2+} in their biochemical measurements, Koch and Stryer (1988) obtained a half-inhibition constant of ~100 nM Ca^{2+} and a Hill coefficient near 4. Using Mg^{2+} concentrations closer to the physiological situation, we found a similar inhibition constant, but a much less steep dependence, with a Hill coefficient of only ~2. This is comparable to the results of Gorczyca et al. (1994*a*) with 1.3 mM (S_p)-GTPαS as substrate and 10 mM total Mg^{2+}; these authors obtained a half-inhibition constant of ~240 nM Ca^{2+} and a Hill coefficient of 2. A lower Hill coefficient has the advantage of providing a broader Ca^{2+} operating range for the enzyme, in contrast to a very steep Ca^{2+} dependence, which would turn a small change in the Ca^{2+} concentration into an "on–off" switch. Biochemical experiments have also shown that the Ca^{2+} modulation of cyclase is mediated by a protein named GCAP, which activates cyclase in the absence of Ca^{2+} (Gorczyca et al., 1994*a*; Palczewski, Subbaraya, Gorczyca, Helekar, Ruiz, Ohguro, Huang, Zhao, Crabb, Johnson, Walsh, Gray-Keller, Detwiler, and Baehr, 1994; Koch and Stryer, 1988). Our results from single cells show a competition between Ca^{2+} and MgGTP. This suggests that the Ca^{2+}-bound activator remains associated with the cyclase and exerts its inhibitory effect by reducing the enzyme's affinity for MgGTP.

For describing the Ca^{2+} modulation of cyclase in the intact cell, the measurements made with a K^+ intracellular solution (Fig. 13) are probably more appropriate. The lack of ATP in these experiments is not significant, since we have found that ATP does not affect the half-inhibition constant for Ca^{2+} (see also Gorczyca et al., 1994*b*). The difference between the modulation in 2 mM GTP/0.5 mM free Mg^{2+} (inhibition constant of ~90 nM Ca^{2+} and Hill coefficient of 2) and that in 0.5 mM GTP/0.5 mM free Mg^{2+} (inhibition constant of ~60 nM Ca^{2+} and Hill coefficient of 1.7) is not very large, so the choice between them is not critical. The total GTP concentration in the outer segment is 1–2 mM (Robinson and Hagins, 1979; Biernbaum and Bownds, 1985). Since there are no known rod outer segment

GTP-binding sites that could bind millimolar concentrations of GTP, we have assumed that most of the GTP is free. The dark Ca^{2+} concentration in the intact rod outer segment has been measured to be 220–550 nM (Ratto, Payne, Owen, and Tsien, 1988; Korenbrot and Miller, 1989; Lagnado et al., 1992; Gray-Keller and Detwiler, 1994; McCarthy et al., 1994). For the 2-mM GTP curve, this Ca^{2+} concentration would give a guanylate cyclase activity in the dark of 1.9–0.3 μM cGMP s^{-1}. In bright light, when the Ca^{2+} concentration might decrease to 50 nM (Gray-Keller and Detwiler, 1994) or even lower (Cervetto et al., 1989; McCarthy et al., 1994), the cyclase activity could increase, according to the same curve, up to ~13 μM cGMP s^{-1}. Thus, light is expected to modulate the cyclase by up to 5–40-fold. This value is consistent with measurements from intact rods (Cornwall and Fain, 1994), as well as with the increase in cGMP flux in toad retinas observed in bright light (Dawis, Graeff, Heyman, Walseth, and Goldberg, 1988).

APPENDIX

We provide justification here for the use of Eq. 9 to measure guanylate cyclase activity. This equation was initially conceived based on homogeneous distributions of cGMP and GTP in the outer segment. In the actual situation, however, longitudinal gradients are expected. Thus, the concentration of GTP should decrease from the open to the closed end due to cyclase activity. At the same time, the concentration of produced cGMP should decrease from the closed to the open end due to loss through diffusion. The diffusion equations for this situation cannot be solved analytically for any arbitrary cyclase activity. Instead, we adopted the approach of specifying a cyclase activity according to our measurements, and used diffusion theory to calculate the empirical cGMP concentration, [cG], as defined by Eq. 8b. We then compared the product r[cG] with the specified cyclase activity for agreement.

The Parameter r

We first relate the parameter r to the cGMP diffusion coefficient, D, in the outer segment and show that [cG] declines exponentially with rate constant r.

Fig. 14 is a schematic diagram of a truncated rod outer segment, with L representing the length and s the seal position (see Koutalos et al., 1995). Longitudinal diffusion in the outer segment is much slower than lateral diffusion because of the baffling by the membranous disks. Thus, we can assume cross-sectional homogeneity in the time scale of longitudinal diffusion and use a one-dimensional diffusion model.

The parameter r is measured from the time course of decline of the cGMP-activated current upon removing cGMP from the dialyzing solution. This situation has been dealt with in a previous paper (Koutalos et al., 1995). It was shown that, under these circumstances, the concentration $G(x,t)$ of cGMP at position x and time t in the outer segment declines according to

$$G(x,t) = \frac{4G_0}{\pi}\sum_{i=0}^{\infty}\left\{\frac{(-1)^i}{(2i+1)}e^{-(2i+1)^2 rt}\cos\frac{(2i+1)\pi x}{2L}\right\}, \qquad \text{(A1)}$$

where G_0 is the initial concentration of cGMP and

$$r = \frac{\pi^2 D}{4L^2}. \tag{A2}$$

The infinite series converges rapidly; we have kept the first six terms for calculations. Since only the part of the outer segment between the seal position and the tip contributes to the measured current, the normalized current from the whole outer segment is given by

$$j(t) = \frac{1}{L-s}\int_0^{L-s} \frac{G(x,t)^n}{G(x,t)^n + K_{1/2}{}^n}\, dx. \tag{A3}$$

The truncated rod outer segment lengths were usually between 20 and 30 μm. For the following calculations we have adopted G_0 = 1 mM cGMP, L = 25 μm, $K_{1/2}$ = 36 μM cGMP, and n = 1.9, and also chosen s = 5 μm on the basis of the results by Nakatani and Yau (1988*b*) from toad rods. However, the final result is not sensitive

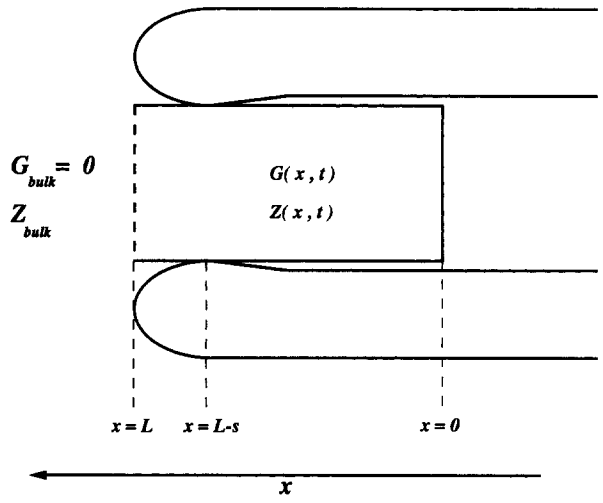

FIGURE 14. Schematic diagram of a truncated rod outer segment for the construction of the diffusion model. The distal, closed end of the outer segment is at x = 0, whereas the proximal, open end is at x = L. Z_{bulk} and G_{bulk} are the bulk concentrations of GTP and cGMP, respectively. In all cases that we consider, G_{bulk} = 0. The suction pipette collects current from the part of the outer segment beyond the effective seal position, located at $L - s$.

to the particular values for L and s. From Eqs. 8b, A1, and A3, we can calculate [cG] as a function of the product rt. In Fig. 15, $\ln\{[cG]/K_{1/2}\}$ is plotted as a function of rt. For [cG] ≤ 5 $K_{1/2}$ (i.e., for [cG] ≤ 180 μM), the relation is a straight line with a slope of unity, showing that [cG] decays exponentially with rate constant r.

For calculations of r[cG] below, we have adopted r = 0.3 s^{-1}, a typical value. For L = 25 μm, we obtain, from Eq. A2, $D = 75 \times 10^{-8}$ cm^2 s^{-1}, a value close to that arrived at previously (Koutalos et al., 1995).

Calculation of [cG]

The equations describing cGMP and GTP diffusion inside the truncated rod outer segment in the presence of a guanylate cyclase activity α are

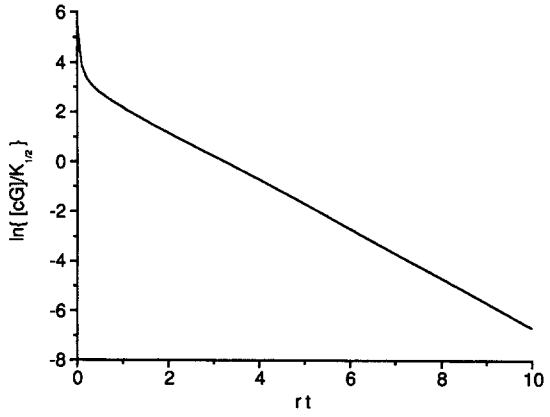

FIGURE 15. Plot of $\ln\{[cG]/K_{1/2}\}$ as a function of rt, where [cG] is the cGMP concentration as defined by Eq. 8b. The relation has a slope of -1 over the experimental concentration range for [cG] (see text), indicating that [cG] decays exponentially with rate constant r.

$$\frac{\partial Z(x,t)}{\partial t} = D\frac{\partial^2 Z(x,t)}{\partial x^2} - \alpha\,[Z(x,t)] \tag{A4}$$

$$\frac{\partial G(x,t)}{\partial t} = D\frac{\partial^2 G(x,t)}{\partial x^2} + \alpha\,[Z(x,t)] \tag{A5}$$

where $Z(x,t)$ and $G(x,t)$ are GTP (or MgGTP) and cGMP concentrations, respectively, at position x and at time t, and $\alpha\,[Z(x,t)]$ is the guanylate cyclase activity as a function of the GTP concentration; the cyclase activity is assumed to be uniform along the length of the outer segment. The diffusion coefficient, D, is assumed to be the same for cGMP and GTP on the basis of their similar molecular weights and the kinetics of their elicited currents (cf. Figs. 2 *A* and 4 *A*). In Eq. A4, the GTPase activity of transducin has been ignored because the experiments were carried out in the dark, whereas the hydrolysis of cGMP by the phosphodiesterase has been ignored in Eq. A5 because of the presence of IBMX. Previous experiments (Koutalos et al., 1995) have indicated that 0.5 mM IBMX is sufficient to inhibit the basal phosphodiesterase activity.

At steady state, the concentrations will be functions of position only, and Eqs. A4 and A5 become

$$D\frac{\partial^2 Z(x)}{\partial x^2} = \alpha\,[Z(x)] \tag{A6}$$

$$D\frac{\partial^2 G(x)}{\partial x^2} = -\alpha\,[Z(x)]\,. \tag{A7}$$

The boundary condition at the closed end is given by the "zero-flux" requirement:

$$\frac{\partial Z(x)}{\partial x} = 0 \qquad \text{at } x = 0 \tag{A8}$$

$$\frac{\partial G(x)}{\partial x} = 0 \qquad \text{at } x = 0, \tag{A9}$$

while at the open end we have

$$Z(L) = Z_{\text{bulk}} \tag{A10}$$

$$G(L) = 0, \tag{A11}$$

where Z_{bulk} is the bulk concentration of GTP in the bath.

With a specified dependence of the guanylate cyclase activity, α, on GTP concentration, Eq. A6 can be solved for $Z(x)$ with boundary conditions A8 and A10. Eq. A7 can then be solved for $G(x)$ with boundary conditions A9 and A11. The normalized, steady state current at a bath GTP concentration Z_{bulk} is then given by

$$j(Z_{\text{bulk}}) = \frac{1}{L-s}\int_0^{L-2} \frac{G(x)^n}{G(x)^n + K_{1/2}^n}\,dx. \tag{A12}$$

Applying this $j(Z_{\text{bulk}})$ to Eq. 8b, [cG] can be calculated. Multiplying with the measured r, we obtain r[cG].

Comparison of α and r[cG]

We have compared the guanylate cyclase activity α and the product r[cG] for the two measured GTP dependencies of the cyclase shown in Fig. 4. Fig. 16 *A* shows an activity α specified according to the data in the presence of 1.6 mM Mg^{2+} and 0 Ca^{2+}, namely, with $V_{\max}$ = 25 μM cGMP s^{-1}, K_m = 250 μM MgGTP, and h = 1.4 (*solid curve*). The circles show the calculated r[cG] at several bath GTP concentrations. A least-squares fit of the Hill equation to these points gives $V_{\max}$ = 31 μM cGMP s^{-1}, K_m = 300 μM MgGTP, and h = 1.4 (*dashed line*), in reasonable agreement with the specified α, except for an overestimation of $V_{\max}$ and K_m by ~20%. Fig. 16 *B* shows a specified activity α according to the data in the presence of 0.5 mM Mg^{2+} and 0 Ca^{2+}, namely, with $V_{\max}$ = 17 μM cGMP s^{-1}, K_m = 310 μM MgGTP, and h = 2.6 (*solid curve*). This relation gives rise to r[cG] values computed at several bath GTP concentrations as indicated by the circles. A least-squares fit of the Hill equation to the points in this case gives $V_{\max}$ = 21 μM cGMP s^{-1}, K_m = 360 μM MgGTP, and h = 2.5 (*dashed line*), again in reasonable agreement with α, except for a similar overestimation of $V_{\max}$ and K_m.

The above comparisons suggest that Eq. 9 provides a reasonable measurement of guanylate cyclase activity under our experimental conditions. Given the cyclase activity as measured, the spatial profiles of the steady state GTP and cGMP concentrations can be calculated. Such an analysis shows that the maximum deviation of the GTP concentration inside the outer segment from the bulk concentration is <20%, decreasing to <10% as the cyclase activity approaches saturation. The cGMP concentration, however, can vary by twofold over the longitudinal part of the outer segment that contributes to the measured current (i.e., the part between the pipette seal and the closed end). Thus, the validity of Eq. 9 does not strictly require spatial uniformity of the cGMP and GTP concentrations along the rod outer seg-

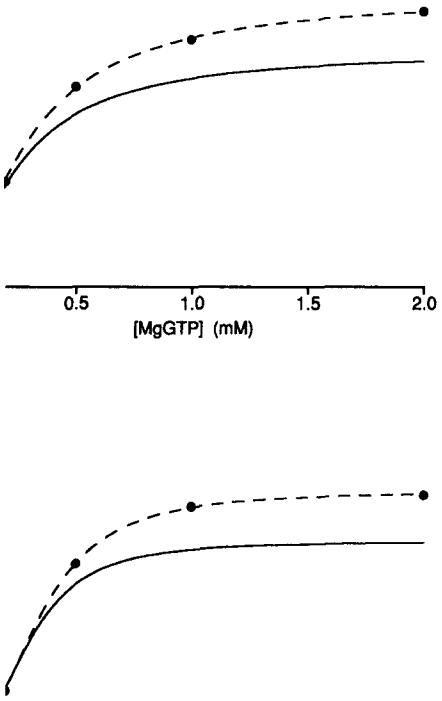

FIGURE 16. Justification of using the relation r[cG] as a measure of guanylate cyclase activity. In both panels, the solid curve represents the specified guanylate cyclase activity α, and the circles (fitted by dashed curve) represent the product r[cG] expected to be measured. See text for details.

ment. On the other hand, Eq. 9 is not necessarily a good measure of the cyclase activity in the general case, either. If the enzyme were far more active, then the supply of MgGTP through diffusion might not have been sufficiently fast to keep up. We find that, as a rule of thumb, Eq. 9 provides a good measure of the cyclase activity when the rate constant r is larger than the ratio V_{max}/K_m. This has been the case for the enzyme studied here.

We thank Dr. R.-C. Huang for helpful discussions.

This work was supported by National Institutes of Health grant EY06837. Y. Koutalos held a postdoctoral fellowship from the Fight for Sight Research Division of Prevent Blindness America, awarded in memory of Mary E. and Alexander P. Hirsch.

Original version received 10 January 1995 and accepted version received 16 May 1995.

REFERENCES

Baylor, D. A., T. D. Lamb, and K.-W. Yau. 1979. The membrane current of single rod outer segments. *Journal of Physiology*. 288:589–611.

Biernbaum, M. S., and M. D. Bownds. 1985. Frog rod outer segments with attached inner segment ellipsoids as an in vitro model for photoreceptors on the retina. *Journal of General Physiology.* 85:83–105.

Cervetto, L., L. Lagnado, R. J. Perry, D. W. Robinson, and P. A. McNaughton. 1989. Extrusion of Ca from rod outer segments is driven by both sodium and potassium gradients. *Nature.* 337:740–743.

Chen, C.-K., and J. B. Hurley. 1994. Calcium-dependent recoverin/rhodopsin kinase interaction. *Investigative Ophthalmology and Visual Science.* 35:1485 (Abstr.)

Chen, J., C. L. Makino, N. S. Peachey, D. A. Baylor, and M. I. Simon. 1995. Mechanisms of rhodopsin inactivation in vivo as revealed by a C-terminal truncation mutant. *Science.* 267:374–377.

Chen, T.-Y., M. Illing, L. L. Molday, Y.-T. Hsu, K.-W. Yau, and R. S. Molday. 1994. Subunit 2 (or β) of retinal rod cGMP-gated channel is a component of the 240 kD channel-associated protein and mediates Ca^{2+}-calmodulin modulation. *Proceedings of the National Academy of Sciences, USA.* 91:11757–11761.

Colamartino, G., A. Menini, and V. Torre. 1991. Blockage and permeation of divalent cations through the cyclic GMP-activated channel from tiger salamander retinal rods. *Journal of Physiology.* 440:189–206.

Cornwall, M. C., and G. L. Fain. 1994. Bleached pigment activates transduction in isolated rods of the salamander retina. *Journal of Physiology.* 480:261–279.

Dawis, S. M., R. M. Graeff, R. A. Heyman, T. F. Walseth, and N. D. Goldberg. 1988. Regulation of cGMP metabolism in toad photoreceptors. *Journal of Biological Chemistry.* 263:8771–8785.

Detwiler, P. B., and M. P. Gray-Keller. 1992. Some unresolved issues in the physiology and biochemistry of phototransduction. *Current Opinion in Neurobiology.* 2:433–438.

Fesenko, E. E., S. Kolesnikov, and A. L. Lyubarsky. 1985. Induction by cyclic GMP of cationic conductance in plasma membrane of retinal rod outer segment. *Nature.* 313:310–313.

Fleischman, D., and M. Denisevich. 1979. Guanylate cyclase of isolated bovine retinal rod axonemes. *Biochemistry.* 18:5060–5066.

Gorczyca, W. A., M. P. Gray-Keller, P. B. Detwiler, and K. Palczewski. 1994*a*. Purification and physiological evaluation of a guanylate cyclase activating protein from retinal rods. *Proceedings of the National Academy of Sciences, USA.* 91:4014–4018.

Gorczyca, W. A., J. P. Van Hooser, and K. Palczewski. 1994*b*. Nucleotide inhibitors and activators of retinal guanylate cyclase. *Biochemistry.* 33:3217–3222.

Gordon, S. E., and A. L. Zimmerman. 1994. Modulation of the rod cGMP-gated ion channel by calmodulin and an endogenous factor distinct from calmodulin. *Biophysical Journal.* 66:A355. (Abstr.)

Gray-Keller, M. P., and P. B. Detwiler. 1994. The calcium feedback signal in the phototransduction cascade of vertebrate rods. *Neuron.* 13:849–861.

Gray-Keller, M. P., A. S. Polans, K. Palczewski, and P. B. Detwiler. 1993. The effect of recoverin-like calcium-binding proteins on the photoresponse of retinal rods. *Neuron.* 10:523–531.

Hakki, S., and A. Sitaramayya. 1990. Guanylate cyclase from bovine rod outer segments: solubilization, partial purification, and regulation by inorganic pyrophosphate. *Biochemistry.* 29:1088–1094.

Hayashi, F., and A. Yamazaki. 1991. Polymorphism in purified guanylate cyclase from vertebrate rod photoreceptors. *Proceedings of the National Academy of Sciences, USA.* 88:4746–4750.

Haynes, L., and K.-W. Yau. 1985. Cyclic GMP-sensitive conductance in outer segment membrane of catfish cones. *Nature.* 317:61–64.

Hsu, Y.-T., and R. S. Molday. 1993. Modulation of the cGMP-gated channel of rod photoreceptor cells by calmodulin. *Nature.* 361:76–79.

Karpen, J. W., R. L. Brown, L. Stryer, and D. A. Baylor. 1993. Interactions between divalent cations and the gating machinery of cyclic GMP-activated channels in salamander retinal rods. *Journal of General Physiology.* 101:1–25.

Kawamura, S. 1993. Rhodopsin phosphorylation as a mechanism of cyclic GMP phosphodiesterase regulation by S-modulin. *Nature.* 362:855–857.

Kawamura, S., and M. Murakami. 1989. Regulation of cGMP levels by guanylate cyclase in truncated frog rod outer segments. *Journal of General Physiology.* 94:649–668.

Kawamura, S., and M. Murakami. 1991. Calcium-dependent regulation of cyclic GMP phosphodiesterase by a protein from frog retinal rods. *Nature.* 349:420–423.

Koch, K.-W. 1991. Purification and identification of photoreceptor guanylate cyclase. *Journal of Biological Chemistry.* 266:8634–8637.

Koch, K.-W., and L. Stryer. 1988. Highly cooperative feedback control of retinal rod guanylate cyclase by calcium ions. *Nature.* 334:64–66.

Korenbrot, J. I., and D. L. Miller. 1989. Cytoplasmic free calcium concentration in dark adapted retinal rod outer segments. *Vision Research.* 29:939–948.

Koutalos, Y., K. Nakatani, and K.-W. Yau. 1992. Guanylate cyclase studied in truncated rod outer segments. *Biophysical Journal.* 61:428*a.* (Abstr.)

Koutalos, Y., K. Nakatani, and K.-W. Yau. 1993. A quantitative account of the role of Ca^{2+} in light adaptation of rod photoreceptors. *Society for Neuroscience Abstracts.* 19:1200. (Abstr.)

Koutalos, Y., K. Nakatani, and K.-W. Yau. 1995. Cyclic GMP diffusion coefficient in rod photoreceptor outer segments. *Biophysical Journal.* 68:373–382.

Koutalos, Y., and K.-W. Yau. 1993. A rich complexity emerges in phototransduction. *Current Opinion in Neurobiology.* 3:513–519.

Lagnado, L., and D. A. Baylor. 1992. Signal flow in visual transduction. *Neuron.* 8:995–1002.

Lagnado, L., and D. A. Baylor. 1994. Calcium controls light-triggered formation of catalytically active rhodopsin. *Nature.* 367:273–277.

Lagnado, L., L. Cervetto, and P. A. McNaughton. 1992. Calcium homeostasis in the outer segments of retinal rods from the tiger salamander. *Journal of Physiology.* 455:111–142.

Lamb, T. D., P. A. McNaughton, and K.-W. Yau. 1981. Spatial spread of activation and background desensitization in toad rod outer segments. *Journal of Physiology.* 319:463–496.

London, R. E. 1991. Methods for measurement of intracellular magnesium: NMR and fluorescence. *Annual Review of Physiology.* 53:241–258.

Martell, A. E., and R. M. Smith. 1974. Critical Stability Constants. Vol. 1. Amino Acids. Plenum Publishing Corp., NY. 469 pp.

Matthews, H. R. 1995. Effects of lowered cytoplasmic calcium concentration and light on the responses of salamander rod photoreceptors. *Journal of Physiology.* 484:267–286.

Matthews, H. R., G. L. Fain, R. L. W. Murphy, and T. D. Lamb. 1990. Light adaptation in cone photoreceptors of the salamander: a role for cytoplasmic calcium. *Journal of Physiology.* 420:447–469.

Matthews, H. R., R. L. W. Murphy, G. L. Fain, and T. D. Lamb. 1988. Photoreceptor adaptation is mediated by cytoplasmic calcium concentration. *Nature.* 334:67–69.

McCarthy, S. T., J. P. Younger, and W. G. Owen. 1994. Free calcium concentrations in bullfrog rods determined in the presence of multiple forms of Fura-2. *Biophysical Journal.* 67:2076–2089.

McNaughton, P. A., L. Cervetto, and B. J. Nunn. 1986. Measurement of the intracellular free calcium concentration in salamander rods. *Nature.* 322:261–263.

Miller, J. L., and J. I. Korenbrot. 1994. Differences in calcium homeostasis between retinal rod and cone photoreceptors revealed by the effects of voltage on the cGMP-gated conductance in intact cells. *Journal of General Physiology.* 104:909–940.

Nakatani, K., Y. Koutalos, and K.-W. Yau. 1995. Ca^{2+} modulation of the cGMP-gated channel of bullfrog retinal rod photoreceptors. *Journal of Physiology.* 484:69–76.

Nakatani, K., and K.-W. Yau. 1985. cGMP opens the light-sensitive conductance in retinal rods. *Biophysical Journal.* 47:356*a.* (Abstr.)

Nakatani, K., and K.-W. Yau. 1988*a*. Calcium and magnesium fluxes across the plasma membrane of the toad rod outer segment. *Journal of Physiology*. 395:695–729.

Nakatani, K., and K.-W. Yau. 1988*b*. Guanosine 3′,5′-cyclic monophosphate-activated conductance studied in a truncated rod outer segment of the toad. *Journal of Physiology*. 395:731–753.

Nakatani, K., and K.-W. Yau. 1988*c*. Calcium and light adaptation in retinal rods and cones. *Nature*. 334:69–71.

Palczewski, K., G. Rispoli, and P. B. Detwiler. 1992. The influence of arrestin (48K protein) and rhodopsin kinase on visual transduction. *Neuron*. 8:117–126.

Palczewski, K., I. Subbaraya, W. A. Gorczyca, B. S. Helekar, C. C. Ruiz, H. Ohguro, J. Huang, X. Zhao, J. W. Crabb, R. S. Johnson, et al. 1994. Molecular cloning and characterization of retinal photoreceptor guanylyl cyclase activating protein. *Neuron*. 13:395–404.

Pugh, E. N., Jr., and T. D. Lamb. 1993. Amplification and kinetics of the activation steps in phototransduction. *Biochimica et Biophysica Acta*. 1141:111–149.

Ratto, G. M., R. Payne, W. G. Owen, and R. Y. Tsien. 1988. The concentration of cytosolic free Ca^{2+} in vertebrate rod outer segments measured with fura 2. *Journal of Neuroscience*. 8:3240–3246.

Robinson, W. E., and W. A. Hagins. 1979. GTP hydrolysis in intact rod outer segments and the transmitter cycle in visual excitation. *Nature*. 280:398–400.

Somlyo, A. P., and B. Walz. 1985. Elemental distribution in Rana pipiens retinal rods: quantitative electron probe analysis. *Journal of Physiology*. 358:183–195.

Tsien, R. Y. 1980. New calcium indicators and buffers with high selectivity against magnesium and protons: design, synthesis, and properties of prototype structures. *Biochemistry*. 19:2396–2404.

Yang, Z., and T. G. Wensel. 1992. Inorganic pyrophosphatase from bovine retinal rod outer segments. *Journal of Biological Chemistry*. 267:24634–24640.

Yarfitz, S., and J. B. Hurley. 1994. Transduction mechanisms of vertebrate and invertebrate photoreceptors. *Journal of Biological Chemistry*. 269:14329–14332.

Yau, K.-W. 1994. Phototransduction mechanism in retinal rods and cones. The Friedenvald Lecture. *Investigative Ophthalmology and Visual Science*. 35:9–32.

Yau, K.-W., and D. A. Baylor. 1989. Cyclic GMP-activated conductance of retinal photoreceptor cells. *Annual Review of Neuroscience*. 12:289–327.

Yau, K.-W., and K. Nakatani. 1984. Electrogenic Na-Ca exchange in retinal rod outer segment. *Nature*. 311:661–663.

Yau, K.-W., and K. Nakatani. 1985*a*. Light-induced reduction of cytoplasmic free calcium in retinal rod outer segment. *Nature*. 313:579–582.

Yau, K.-W., and K. Nakatani. 1985*b*. Light-suppressible, cyclic GMP-sensitive conductance in the plasma membrane of a truncated rod outer segment. *Nature*. 317:252–255.

Zimmerman, A. L., and D. A. Baylor. 1992. Cation interactions within the cyclic GMP-activated channel of retinal rods from the tiger salamander. *Journal of Physiology*. 449:759–783.

Zimmerman, A. L., G. Yamanaka, F. Eckstein, D. A. Baylor, and L. Stryer. 1985. Interaction of hydrolysis-resistant analogs of cyclic GMP with the phosphodiesterase and light-sensitive channel of retinal rod outer segments. *Proceedings of the National Academy of Sciences, USA*. 82:8813–8817.